

## Neurobiology

# Causal Role of Apoptosis-Inducing Factor for Neuronal Cell Death Following Traumatic Brain Injury

Jennifer E. Slemmer,<sup>\*†</sup> Changlian Zhu,<sup>‡</sup>  
Stefan Landshamer,<sup>§</sup> Raimund Trabold,<sup>¶</sup>  
Julia Grohm,<sup>||</sup> Ardavan Ardeshiri,<sup>¶</sup> Ernst Wagner,<sup>§</sup>  
Marva I. Sweeney,<sup>\*</sup> Klas Blomgren,<sup>##</sup>  
Carsten Culmsee,<sup>§\*\*</sup> John T. Weber,<sup>†,††</sup>  
and Nikolaus Plesnila<sup>¶##</sup>

From the Department of Biology,<sup>\*</sup> University of Prince Edward Island, Charlottetown, Prince Edward Island, Canada; Department of Neuroscience,<sup>‡</sup> Erasmus Medical Center, Rotterdam, The Netherlands; Center for Brain Repair and Rehabilitation,<sup>§</sup> Institute of Neuroscience and Physiology, University of Gothenburg, Sweden; Pharmaceutical Biology-Biotechnology,<sup>§</sup> Department of Pharmacy, University of Munich, Germany; Department of Neurosurgery & Institute for Surgical Research,<sup>¶</sup> University of Munich Medical Center-Großhadern, Germany; Department of Pediatric Oncology,<sup>||</sup> The Queen Silvia Children's Hospital, University of Gothenburg, Sweden; Institute for Pharmacology and Toxicology,<sup>\*\*</sup> Philipps University Marburg, Germany; School of Pharmacy,<sup>††</sup> Memorial University of Newfoundland, St. John's, Newfoundland, Canada; Department of Physiology and Neurodegeneration,<sup>##</sup> Royal College of Surgeons in Ireland, Dublin Ireland

**Traumatic brain injury (TBI) consists of two phases: an immediate phase in which damage is caused as a direct result of the mechanical impact; and a late phase of altered biochemical events that results in delayed tissue damage and is therefore amenable to therapeutic treatment. Because the molecular mechanisms of delayed post-traumatic neuronal cell death are still poorly understood, we investigated whether apoptosis-inducing factor (AIF), a pro-apoptotic mitochondrial molecule and the key factor in the caspase-independent, cell death signaling pathway, plays a causal role in neuronal death following TBI. Using an *in vitro* model of neuronal stretch injury, we demonstrated that AIF translocated from mitochondria to the nucleus of neurons displaying axonal disruption, chromatin condensation, and nuclear pyknosis in a caspase-independent manner, whereas astrocytes remained unaffected. Similar findings were observed following experimental TBI in mice, where AIF translocation to the nucleus coincided with delayed**

**neuronal cell death in both cortical and hippocampal neurons. Down-regulation of AIF *in vitro* by siRNA significantly reduced stretch-induced neuronal cell death by 67%, a finding corroborated *in vivo* using AIF-deficient harlequin mutant mice, where secondary contusion expansion was significantly reduced by 44%. Hence, our current findings demonstrate that caspase-independent, AIF-mediated signaling pathways significantly contribute to post-traumatic neuronal cell death and may therefore represent novel therapeutic targets for the treatment of TBI. (Am J Pathol 2008, 173:1795–1805; DOI: 10.2353/ajpath.2008.080168)**

Traumatic brain injury (TBI) is the most common cause of death in children and young adults in industrialized countries.<sup>1</sup> Among the various pathologies associated with TBI, gray and white matter contusions are the most frequent focal abnormalities associated with high mortality and unfavorable functional outcome.<sup>2</sup> The pathophysiology of cerebral contusions is characterized by complex regional and temporal changes of cerebral blood flow and metabolism,<sup>3,4</sup> disruption of the blood brain barrier resulting in brain edema formation,<sup>5</sup> and cell death signaling,<sup>6–8</sup> finally leading to progressive neuronal cell death in pericontusional tissue (ie, the traumatic penumbra).<sup>9</sup> The macroscopic manifestation of pericontusional cell death is a delayed increase of contusion volume over time,<sup>10</sup> a finding termed “secondary contusion expansion,” and recently characterized experimentally in detail.<sup>11</sup>

The ultimate steps leading to delayed cell death in pericontusional tissue are initiated by a combination of multiple mechanisms, such as over-activation of glutamate receptors,<sup>12</sup> free radical-mediated membrane damage,<sup>13</sup> nuclear translocation of transcription factors,<sup>14</sup> expression and up-regulation of inflammatory media-

Supported by the Fakultätsförderprogramm für Forschung und Lehre (FöFoLe) of the University of Munich, a Breedtestrategie subsidie from Erasmus MC, the Swedish Research Council, the Swedish Childhood Cancer Foundation and Hersenstichting Nederland.

Accepted for publication September 3, 2008.

Address reprint requests to Prof. Nikolaus Plesnila, M.D., Ph.D., Royal College of Surgeons in Ireland (RCSI), 123 St. Stephens Green, Dublin 2, Ireland. E-mail: nikolausplesnila@rcsi.ie.

tors,<sup>15</sup> and activation of apoptosis-like cell death signaling pathways.<sup>8,16,17</sup> Accumulating evidence suggests that the activation of caspases<sup>18,19</sup> by oligomerization of cell membrane-bound death receptors,<sup>20,21</sup> regulation of bcl-2 family proteins,<sup>22</sup> and the release of pro-apoptotic proteins from mitochondria<sup>23,24</sup> are the prominent signaling pathways that cause DNA fragmentation and pericontusional cell death. While caspase-dependent cell death signaling via the release of cytochrome c from mitochondria, followed by apoptosome formation and activation of effector caspases 3, 6, and possibly 7, have been studied in detail,<sup>25,26</sup> little is known about the contribution of the recently described caspase-independent signaling pathway<sup>27</sup> for post-traumatic neuronal cell death. So far, apoptosis-inducing factor (AIF) has only been shown to translocate to the nucleus following a combination of traumatic brain injury and hypoxemia in rats.<sup>28</sup> However, since hypoxia alone also results in AIF-mediated cell death,<sup>29</sup> the role of AIF in traumatic neuronal cell death remained unclear. The aim of the current study was therefore to investigate the role of the caspase-independent pro-apoptotic mitochondrial protein AIF. To that end, we used *in vitro* and *in vivo* models for traumatic cell death, together with anti-AIF siRNA and functionally AIF-deficient mice, to characterize the role of AIF in pericontusional cell death.

## Materials and Methods

### Cell Culture

Primary cortical or hippocampal cell cultures were prepared from E18 wild-type FVB/N mouse embryos as previously described.<sup>30</sup> Briefly, dissociated cortices or hippocampi were diluted in serum-containing media [Basal Medium Eagles (Invitrogen, Carlsbad, CA) containing 10% horse serum (GIBCO), 10  $\mu$ g/ml gentamicin (Sigma, St. Louis, MO), 0.5% glucose (Sigma), 1 mmol/L sodium pyruvate (Invitrogen), and 1% N2 supplements (Invitrogen)] to a concentration of 500,000 cells per ml; cells were then plated in 1 ml aliquots onto collagen-coated six-well FlexPlates (FlexCell, Hillsborough, NC) coated overnight with poly-L-ornithine (500  $\mu$ g/ml; Sigma). All cultures were maintained in a humidified incubator (5% CO<sub>2</sub>, 37°C). Neuronally enhanced cultures were obtained by replacing half of the media 2 days after plating, and then twice per week, with serum-free media containing 2% B27 supplements (Invitrogen). Glia formed a confluent monolayer that adhered to the membrane substrate, while neurons grew in the upper layer of cultures that adhered to the underlying glial layer.

### Immunocytochemistry

Immunohistochemistry was performed as previously described.<sup>30,31</sup> Briefly, cultures were fixed with 4% paraformaldehyde (all steps conducted at room temperature), permeabilized with 0.2% Triton X-100, and then incubated with primary antibodies [anti-AIF (1:200; Santa Cruz Biotechnology, Santa Cruz, CA); anti-microtubule associated

protein 2 (MAP-2; 1:500; Sigma); anti-glial fibrillary acidic protein (1:300; Dakopatts, Glostrup, Denmark)]; polyclonal anti-cytochrome oxidase-antibody (CytOx; 1:200; Cell Signaling, Danvers, MA) for 1 hour, followed by incubation with secondary antibodies (Alexa 488 donkey-anti-goat, Invitrogen, 1:300; Alexa-594-conjugated goat-anti-mouse, 1:300, both Molecular Probes, Eugene, OR; Cy3 goat-anti-rabbit, 1:200, Jackson ImmunoResearch Laboratories, West Grove, PA; Texas red-conjugated goat anti-rabbit, 1:200, Vector Laboratories, Burlingame, CA) for 1 hour. Cultures were dehydrated with ethanol and mounted with 4,6-diamidino-2-phenylindole (DAPI) for nuclear staining (Vector Laboratories, Burlingame, CA). Images were captured using a confocal laser scanning microscope (Carl Zeiss, Jena, Germany) with a  $\times$ 40 or  $\times$ 60 oil immersion objective (351 to 364 nm excitation and 385 to 470 nm band pass emission for detection of DAPI; 488 excitation and 505 to 550 nm band pass emission for green fluorescence; and 543 nm excitation and 560 long pass emission for red fluorescence). All images of one experiment were acquired using the same laser intensities and photodetector gain for the respective settings to allow comparisons of relative levels of immunoreactivity between the different treatment conditions. At least six images of each group were taken by an evaluator blinded to the experimental conditions.

### In Vitro Cell Injury Model

Cultured cells were injured using a well-characterized and established *in vitro* model for traumatic brain injury (94A Cell Injury Controller; Bioengineering Facility, Virginia Commonwealth University, Richmond, VA) as previously described.<sup>30,32,33</sup> In brief, the Silastic membrane of the FlexPlate well was rapidly and transiently deformed by a 50-ms pulse of compressed nitrogen, which deformed the Silastic membrane and adherent cells to varying degrees controlled by pulse pressure. The extent of cell injury—produced by deforming the Silastic membrane on which the cells are grown—was dependent on the degree of deformation, or stretch. Previous work conducted using rat cortical neurons and glia<sup>32,34,35</sup> and mouse hippocampal neurons<sup>30</sup> have characterized three levels of cell stretch (5.5 mm, 6.5 mm, and 7.5 mm deformations), defined as mild, moderate, and severe injury, which result in membrane deformation and biaxial strain or stretch of 31%, 38%, and 54%, respectively. This range of cell stretch has been shown to be relevant to what would occur in humans after rotational acceleration/deceleration injury.<sup>32</sup> We have previously shown that severe injury (7.5 mm deformation) to hippocampal cells results in a high level of cell death and a large number of neurons detaching from the Silastic membrane<sup>30</sup>; therefore, in the present report, cells were subjected to mild (5.5 mm deformation) or moderate injury (6.5 mm deformation) only. Uninjured control wells were contained in the same FlexPlates as injured wells, and thus underwent the same manipulations, except that they did not receive rapid deformation of the Silastic membrane.

### Small Inhibitory RNA for AIF

Cultures were transfected with either AIF small inhibitory (siRNA) [final concentrations: 20 nmol/L (cortical cultures); 10 nmol/L (hippocampal cultures)] or mutant RNA (final concentration: 20 nmol/L) using Lipofectamine 2000 (Invitrogen) mediated delivery as previously described.<sup>36</sup> Briefly, an AIF cDNA template (750 bp) for T7-RNA polymerase *in vitro* transcription was generated from mouse or rat mRNA by reverse transcription (RT)-PCR using the following primers: forward, 5'-GCGTAATACGACTCATATAGGGAGATCCAGGCAACTTGTTCAGC-3'; and reverse, 5'-GCGTAATACGACTCACTATAGGGAGACCTCTGCTCCAGCCCTATCG-3' (initial denaturation at 95°C for 2 minutes; 28 to 30 cycles of 30 seconds 95°C, 1 minute 57°C, and 2 minutes 72°C; and final extension at 70°C for 10 minutes). The cDNA template was precipitated and purified, and *in vitro* transcription was performed by using the TurboScript-T7-Transcription kit (Gene Therapy Systems). The resulting double-stranded RNA template was then exposed to the recombinant Dicer enzyme at 37°C for 16 hours overnight, and the siRNA fragments were again purified on the RNA Purification Columns 1 and 2 of the manufacturer (Gene Therapy Systems). 5'-AAGAGAAAAAGCGAAGAGCCA-3' was used as non-functional mutant RNA. For transfection, the cell culture medium was removed from the wells and replaced with 900  $\mu$ l of transfection media [Basal Medium Eagles (Invitrogen) containing 10% horse serum (Invitrogen), 0.5% glucose (Sigma), 1 mmol/L sodium pyruvate (Invitrogen), and 1% N2 supplements (Invitrogen)]. Transfected control wells and transfected injured wells received AIF siRNA and mutant RNA diluted in Opti-MEM (Invitrogen). Control wells and injured control wells were treated with 2  $\mu$ l Lipofectamine 2000 and Opti-MEM only. All cultures were incubated for 48 hours, after which the cells were injured and were used 4 to 24 hours later for cell viability, immunohistochemistry, RT-PCR, or Western blot analysis (see below).

### Inhibition of Caspase by zVAD

Cultures were transfected with AIF siRNA, or remained untransfected, for 48 hours as described above. The broad-spectrum caspase inhibitor, zVAD (Alexis Biochemicals; San Diego, CA), was dissolved in dimethyl sulfoxide before being diluted 1:1000 in transfection media (final concentration: 50  $\mu$ M), and added to cells at 30 minutes pre-injury.

### Western Blot Analysis

Western blot analysis was performed as described previously.<sup>36-38</sup> Briefly, the blot was probed with an affinity-purified goat polyclonal antibody raised against a peptide mapping the C terminus of mouse AIF (1:500; sc-9416; Santa Cruz) at 4°C overnight. Membranes were then exposed to a rabbit anti-goat horseradish peroxidase-conjugated secondary antibody (1:5000; Vector Laboratories), followed by enhanced chemiluminescence detection of an-

tibody binding (ECL; Amersham Biosciences, Arlington Heights, IL). Equal protein loading was demonstrated by stripping and re-probing the membrane with a monoclonal anti- $\beta$ -actin antibody (AC-15; 1:10,000; Santa Cruz) and a secondary anti-mouse horseradish peroxidase-conjugated antibody (Vector Laboratories).

### RT-PCR

Total RNA was extracted from cells (Nucleospin RNA II kit, Macherey-Nagel, Düren, Germany), and RT-PCR was performed as previously described.<sup>39</sup> Primers for AIF were: forward, 5'-GCGTAATACGACTCACTATAGGGAGATCCAGGCAACTTGTTCAGC-3', and reverse, 5'-GCGTAATACGACTCACTATAGGGAGACCTCTGCTCCAGCCCTATCG-3'. PCR for AIF was performed as follows: initial denaturation at 95°C for 2 minutes; amplification by 28 to 30 cycles of 30 seconds 95°C, 1 minute 57°C, and 2 minutes 72°C; and final extension at 70°C for 10 minutes. Primers for glyceraldehyde-3-phosphate dehydrogenase (GAPDH) were: forward, 5'-CGTCTTCCACCACCATGGAGAAGGC-3', and reverse, 5'-AAGGCCATGCCAGTGAGCTTCCC-3', and PCR for GAPDH was performed as follows: initial denaturation at 95°C for 2 minutes; amplification by 26 cycles of 30 seconds 95°C, 1 minute 57°C, and 2 minutes 70°C, and a final extension at 70°C for 10 minutes. RT-PCR products were visualized under UV illumination after electrophoresis on a 1.5% agarose gel containing ethidium bromide.

### Cell Viability

Cell injury was assessed in cultured cells using the two dyes fluorescein diacetate (FDA; Sigma) and propidium iodide (PI; Sigma) as previously described.<sup>30,33</sup> Images were captured using Texas Red and fluorescein isothiocyanate (FITC; green) filters on either a Leica DMRBE fluorescence microscope equipped with a Hamamatsu C4880 CCD camera, or on a Zeiss AxioScope equipped with an AxioCam CCD camera. FDA and PI images were taken separately, pseudocolored, and overlaid. Cells in five contiguous  $\times$ 100 images were counted and averaged per well. All images were taken from the center portion of the well, as this region was previously shown to receive equal impact from the cell injury controller.<sup>32</sup> All PI and FDA cell counting was performed blind. In control cultures, PI staining was low, accounting for less than 5% of total cell number, consistent with previous reports.<sup>30,33</sup> Final results are expressed as percentage of control values. All experiments were completed using at least two separate culture preparations at 10 to 13 DIV.

### Traumatic Brain Injury in Vivo (Controlled Cortical Impact)

Male C57BL/6 mice (body weight 25 to 28 g, Charles River) or Harlequin mice and their wild-type littermates (Jackson Laboratories) were subjected to controlled cor-

tical impact (CCI) as previously described.<sup>11,14,40</sup> Animals were anesthetized in a halothane chamber (4%). Anesthesia was maintained with a face mask using 1.2% halothane, 30% O<sub>2</sub>, and 69% N<sub>2</sub>O. Body temperature during anesthesia was kept constant at 37.0°C by a feedback controlled heating pad. After induction of anesthesia the skull was fixed in a stereotactic frame and a large craniotomy was performed above the right parietal cortex between the sagittal, the lambdoid, and the coronal sutures and the insertion of the temporal muscle with a high speed drill under continuous cooling with saline. Special attention was paid to leave the dura mater intact. Controlled cortical impact was performed perpendicular to the surface of the brain. The diameter of the impactor tip was 3 mm, the impact velocity 8 m/s, impact duration 150 ms, and the displacement of the brain was 1.0 mm. In sham operated animals (control group) the craniotomy was closed with the initially removed bone flap and conventional tissue glue (Histoacryl, Braun-Melsungen, Melsungen, Germany) without trauma application. The skin over the craniotomy was carefully closed and animals were transferred to an incubator heated to 35°C until recovery of spontaneous motor activity. Mice ( $n = 6$  each group) were sacrificed at 15 minutes, and 2, 6, 12, and 24 hours after CCI by perfusion-fixation under deep halothane anesthesia, and brains were prepared for immunohistochemical analysis.

Brains of Harlequin mice and wild-type littermates ( $n = 6$  to 11 per group) were removed 15 minutes or 24 hours after CCI and flash frozen. Fourteen coronal sections (10  $\mu\text{m}$ ) 500  $\mu\text{m}$  apart from each other were prepared and stained with cresyl violet. Contusion volume was calculated by multiplying contusion areas with the distance between sections.

All procedures described are in concordance with local laws and were approved by the animal protection committee of the Government of Upper Bavaria (protocol number 118/05).

### *Immunohistochemistry*

Animals were perfusion-fixed with 4% paraformaldehyde. Brains were carefully removed and postfixed in 4% paraformaldehyde no longer than 24 hours. After dehydration, the tissue was embedded in paraffin and 5- $\mu\text{m}$  coronal sections from six levels at equal distances (800  $\mu\text{m}$ ) from the rhinencephalon to the cerebellum were prepared on conventional glass slides coated with amino-propyl-triethoxy-silane (Merck, Darmstadt, Germany).

#### *Apoptosis-Inducing Factor and NeuN*

Immunohistochemistry was performed as described previously.<sup>36,37,41</sup> Briefly, non-specific antibody binding was blocked for 30 minutes with 4% horse serum in PBS and endogenous peroxidase activity was blocked with 3% H<sub>2</sub>O<sub>2</sub> in PBS for 5 minutes. Antibodies directed against AIF (2  $\mu\text{g}/\text{ml}$ , sc-9416, Santa Cruz) or NeuN (1:200, 5  $\mu\text{g}/\text{ml}$ ; clone: MAB377, Chemicon, Temecula, CA) were applied to coronal brain sections in Tris-buffered saline containing 1% bovine serum albumen and 0.1% Triton X-100, incubated for 60 minutes at room

temperature. For signal amplification a biotinylated horse anti-goat antibody (6  $\mu\text{g}/\text{ml}$  in PBS) was applied for 60 minutes. Visualization was performed using a Vectastain ABC Elite kit with 0.5 mg/ml 3,3'-diaminobenzidine enhanced with 15 mg/ml ammonium nickel sulfate, 2 mg/ml  $\beta$ -D-glucose, 0.4 mg/ml ammonium chloride, and 0.01 mg/ml  $\beta$ -glucose oxidase (Vector Laboratories). Negative controls, where the primary antibody was omitted, were completely blank. Preabsorption of the anti-AIF antibody with the peptide provided by the manufacturer abolished staining.

#### *Double Labeling of Apoptosis-Inducing Factor and NeuN*

AIF staining was performed as above. After incubation with the AIF antibody and washing, the sections were incubated with Alexa Fluor 594 conjugated horse anti-goat IgG (2  $\mu\text{g}/\text{ml}$ ) diluted in PBS for 60 minutes at room temperature. After washing, NeuN staining was performed by incubating with NeuN antibody (1:200, 5  $\mu\text{g}/\text{ml}$ , clone MAB 377, Chemicon, Temecula, CA) for 60 minutes at room temperature. After washing, the sections were incubated with Alexa Fluor 488 conjugated horse anti-mouse antibody (2  $\mu\text{g}/\text{ml}$ , Vector Laboratories) diluted in PBS for 60 minutes. Finally, sections were incubated with the nuclear stain Hoechst 33342 (Molecular Probes, Eugene, OR), 1  $\mu\text{g}/\text{ml}$  in PBS for 10 minutes at room temperature with gentle agitation, washed and mounted using Vectashield mounting medium (Vector Laboratories, Burlingame, CA).

#### *Hoechst 33342*

After washing, the sections were incubated with 1  $\mu\text{g}/\text{ml}$  Hoechst 33342 in PBS (Molecular Probes, Eugene, OR) for 10 minutes at room temperature with gentle agitation. Thereafter sections were washed, and mounted using Vectashield mounting medium (Vector Laboratories).

#### *Quantification of Nuclear AIF Translocation in Vivo*

Cell counting was performed in areas of cortex affected by trauma by an observer naïve to treatment. From each individual brain ( $n = 5$ ), three sections (100  $\mu\text{m}$  apart) from the region of maximal contusion extension were evaluated. Three visual fields (one visual field = 0.196 mm<sup>2</sup>) were randomly chosen from the traumatic penumbra, and cells were counted within each section. The counts are reported as the average number of cells per section.

#### *Statistical Analysis*

##### *In Vitro Experiments*

Data were analyzed using the statistical program GB Stat (Dynamic Microsystems, Silver Spring, MD) and computed as mean  $\pm$  SEM values. Statistical significance was established by one-way analysis of variance (analysis of variance) followed by Fisher's protected least

significant difference test. Data are considered significant at  $P < 0.05$ .

### In Vivo Experiments

All data are given as mean  $\pm$  SD. For statistical comparisons between groups, the Kruskal-Willis one-way analysis of variance on ranks test was used followed by Dunnett's all pairwise multiple comparison procedure as *post hoc* test. Calculations were performed using a standard statistical software package (SigmaStat 2.0, Jandel Scientific, Erkrath, Germany). Data are considered significant at  $P < 0.05$ .

## Results

### Nuclear Translocation of AIF after Mild and Moderate Stretch Injury in Primary Cultured Mouse Neurons

Primary mouse hippocampal neurons show strong AIF immunoreactivity in the cytoplasm as demonstrated by AIF and MAP-2 double immunostaining (Figure 1A, upper panel). Further colabeling of AIF and cytochrome oxidase (CytOx), a well known mitochondrial marker protein, demonstrated almost exclusive mitochondrial localization of AIF (Figure 1A, lower panel). Four hours after exposure to mild (5.5 mm) or moderate (6.5 mm) stretch injury, the cells were fixed and immunostaining was performed to analyze nuclear AIF translocation in the different injury groups. Strong AIF immunoreactivity colocalized well with MAP-2 staining in double labeling experiments, and AIF staining was always more pronounced in neurons than in the underlying astrocytes (Figure 1B, control). Strikingly, AIF staining in nuclei was detectable in neurons within 4 hours after both mild and moderate stretch injury, and nuclear AIF was observed in the same cells showing dendrite fragmentation, a feature typical for traumatic injury in this model (Figure 1B, 5.5 and 6.5 mm). Similar results were obtained in cortical neurons that also displayed early AIF translocation within a few hours after stretch injury, and double labeling studies in both culture systems revealed that damaged neurons with nuclear translocation of AIF also showed a pronounced reduction of MAP-2 staining (data not shown). It is important to note that astrocytes did not show visible signs of cell damage after stretch injury, and that there was no AIF translocation to the nuclei detectable after moderate or mild stretch injury in these glial cells (Figure 1C).

### AIF Knock Down after siRNA Treatment Significantly Attenuates Neuronal Death after Stretch Injury

In cultured mouse neurons, incubation with AIF-siRNA significantly reduced levels of AIF mRNA and protein within 48 hours compared to controls either treated with vehicle (LF 2000) or non-functional siRNA (mutRNA) as

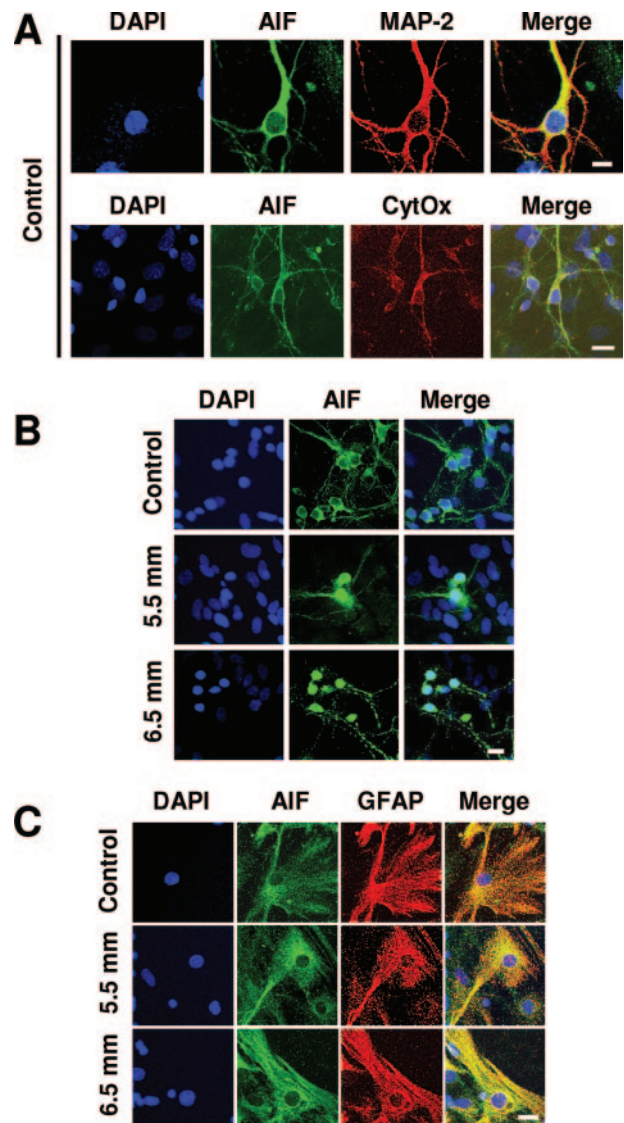


**Figure 1.** AIF translocation after stretch injury in cultured neurons. **A:** Immunocytochemistry and fluorescence confocal laser scanning microscopy revealed pronounced mitochondrial AIF immunoreactivity (green) in cultured embryonic mouse hippocampal neurons labeled with MAP-2 antibodies (red, upper panel) or cytochrome oxidase (CytOx, red, lower panel). The nuclei were labeled with DAPI (blue). **B:** Four hours after mild (5.5 mm) or moderate (6.5 mm) injury, AIF immunoreactivity was clearly detectable in the nuclei of injured neurons as compared to the cytosolic/mitochondrial distribution of AIF in control cultures. The merged pictures show clear overlapping of AIF staining (green) and nuclear DAPI-staining (blue) in injured neurons. Strikingly, neurons with AIF translocation after more severe damage (6.5 mm) also expose clear signs of dendritic fragmentation typical for stretch injury *in vitro*. The underlying astrocyte layer shows less AIF immunoreactivity than the overlying neurons. **C:** AIF immunoreactivity (green) in glial fibrillary acidic protein-positive astrocytes (red) was less pronounced than in neurons, and neither mild (5.5 mm) nor moderate (6.5 mm) stretch injury was able to induce nuclear AIF translocation. AIF remained outside the nuclei (blue) in glial cells. Scale bar = 20  $\mu$ m.

analyzed by PCR, Western blot, or immunocytochemistry (Figure 2, A and B). Cell survival and cell damage were determined at 24 hours after mild or moderate stretch injury by FDA staining and PI uptake, respectively. Mild stretch injury only modestly affected cell survival ( $13 \pm 10\%$  reduction of FDA-positive cells; Figure 2C, left open bar), and increased the percentage of PI-positively

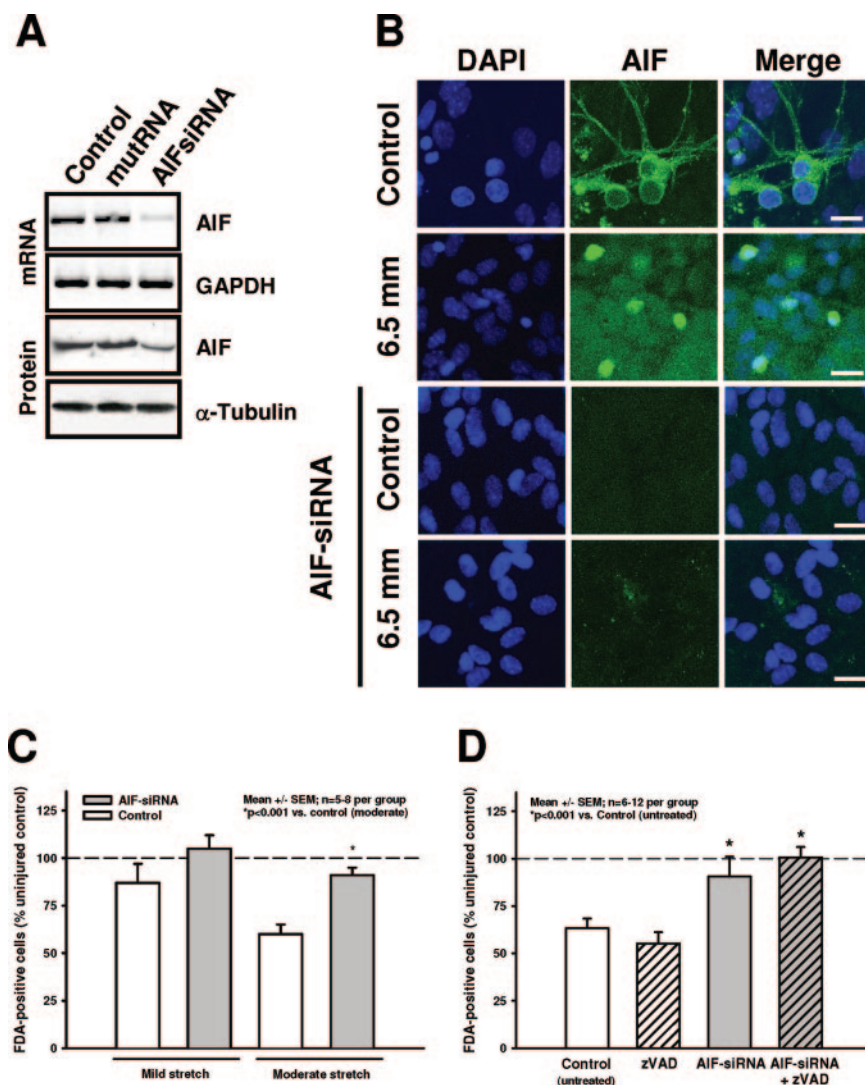


**Figure 2.** Down-regulation of AIF by siRNA prevents stretch-induced injury in cultured neurons. Cultured embryonic mouse neurons were exposed to AIF-siRNA, non-functional siRNA (mutRNA), or vehicle controls (LF 2000) for 48 hours, before extraction of mRNA and protein and/or stretch injury. **A:** RT-PCR (top) and Western blot analysis (bottom) revealed significant siRNA-mediated knock down of AIF mRNA and protein, respectively. GAPDH RT-PCR and  $\alpha$ -tubulin were used as controls to demonstrate specificity of the siRNA effect and equal loading of the gels. **B:** Immunocytochemistry of AIF together with nuclear staining with DAPI revealed strong AIF staining in the cytoplasm and in the nucleus of not injured (control) and injured (6.5 mm) neurons, respectively. Cells treated with AIF-siRNA did not show any AIF staining; neither in the cytoplasm of not injured cells (control) nor in the nucleus of injured cells (6.5 mm). Of note, injured neurons pretreated with AIF-siRNA show normal nuclear morphology. Scale bar: 20  $\mu$ m. **C:** Cell survival was determined at 24 hours after mild or moderate stretch injury by fluorescein diacetate (FDA) staining. Mild stretch only slightly reduced cell survival in the controls (open bars), whereas AIF-siRNA-treated cells (gray bars) did not show any reduction of FDA-stained cells. By contrast, moderate stretch significantly reduced the percentage of FDA-positive cells, and this damage was blocked by pretreatment with AIF-siRNA. (\* $P < 0.001$  as compared to moderately stretched controls;  $n = 5$  to 8 per group). **D:** Cell survival determined by FDA staining following moderate stretch injury (6.5 mm) in untreated control cells (open bar), cells pretreated with the pan-caspase inhibitor zVAD, AIF-siRNA, or both. Caspase inhibition did not show any neuroprotective effect, while down-regulation of AIF prevented stretch-induced neuronal cell death almost completely. zVAD and AIF-siRNA co-treatment did not show any additive effect (\* $P < 0.001$  vs. control;  $n = 6$  to 12 per group).

stained neurons to  $180 \pm 20\%$  of uninjured controls ( $P < 0.01$ ; data not shown). RNAi-mediated AIF knockdown preserved neuronal survival (FDA-positive cells; Figure 2C, left gray bar) at control levels and the increase in PI-positive cells was less pronounced than in the controls (data not shown). By contrast, neurons exposed to moderate stretch showed significant damage, and cell survival (FDA-positive cells) was significantly reduced to  $60 \pm 5\%$  of controls (Figure 2C, right open bar), and the percentage of PI-positive cells increased to  $271 \pm 40\%$  ( $P < 0.01$ ). Cells treated with AIF siRNA and then subjected to moderate stretch showed a clear and significant neuroprotective effect, promoting cell survival almost to levels of uninjured controls as shown by FDA staining (Figure 2C, right gray bar). Moreover, the percentage of PI-positive cells was significantly reduced by 56% from 271 to 175% injured cells in AIF siRNA-treated cells. These results indicate that most of the cell death that occurred after moderate stretch was mediated by AIF.

### *AIF-Mediated Neuronal Cell Death Is Independent of Caspase Activation*

Inhibition of caspases by the pan-caspase inhibitor zVAD did not show any neuroprotective effect following neuronal stretch injury, while down-regulation of AIF preserved neuronal viability almost completely (Figure 2D). Caspase inhibition together with down-regulation of AIF by siRNA did not have any additive effect. These findings confirm our results presented in Figure 2C and support the hypothesis that AIF-mediated cell death is caspase-independent and responsible for a large proportion of stretch-induced neuronal damage.

### *Nuclear Translocation of AIF after Experimental Traumatic Brain Injury in Vivo*

In normal, non-injured cerebral cortex and hippocampus AIF is localized in the cytoplasm (Figures 3A and 4A,

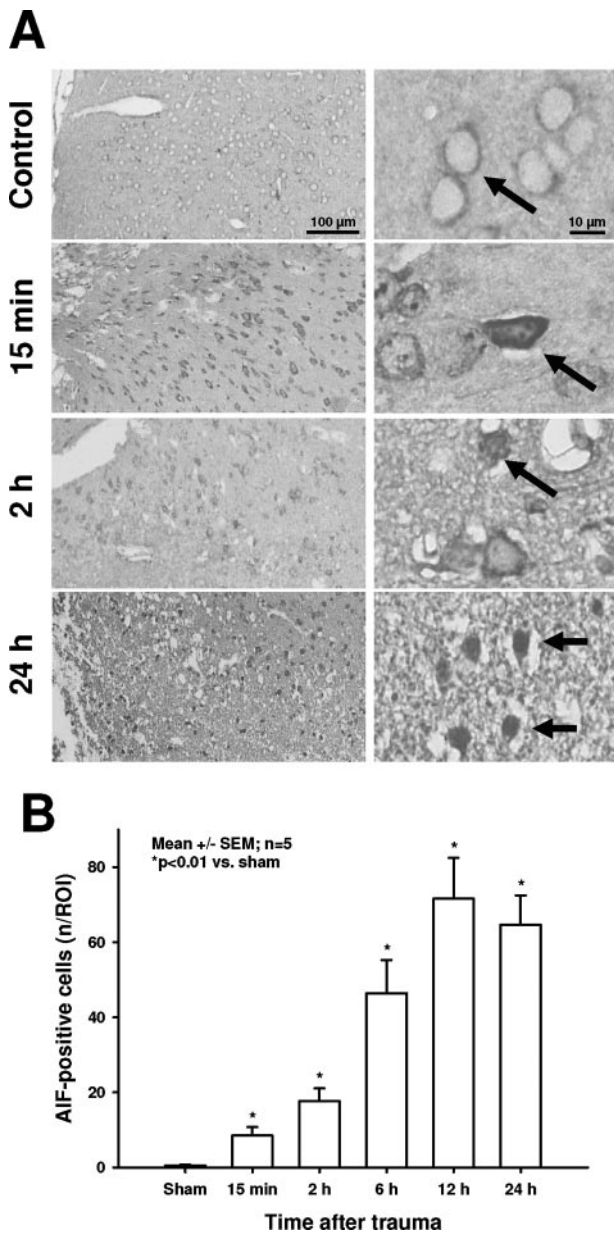


**Figure 3.** Nuclear translocation of AIF in the cerebral cortex following experimental TBI. **A:** Low (left) and high power (right) photomicrographs from control (upper panels) and traumatized brains. AIF (dark staining; arrow) is detected in the cytoplasm of control neurons (Control). At 15 minutes after trauma, the intensity of AIF staining (arrows) increases in the cytoplasm, as well as around the nucleus. At 2 hours after TBI, nuclear morphology is not conspicuously altered. At 24 hours after CCI, most cells showing nuclear AIF staining (arrow) appear shrunken with serrated nuclei, indicating irreversible nuclear damage. **B:** Quantification of neurons (mean  $\pm$  SD) showing nuclear AIF staining (AIF positive) at different time points after TBI. At 15 minutes after trauma, the number of AIF-positive cells is significantly increased as compared to the non-injured brain ( $*P < 0.01$ ;  $n = 5$  per time point). The number of AIF-positive cells continues to increase, reaching maximum values at 12 to 24 hours after TBI.

control) and cannot be found in the nucleus, as demonstrated by double-staining for AIF and a nuclear marker, Hoechst 33342 (Figure 5, AIF+Hoe). As previously shown, the cytoplasmic localization of AIF co-localized with cytochrome oxidase IV staining, a mitochondrial marker, thereby demonstrating that AIF is localized in mitochondria not only *in vitro* but also in the intact brain *in*

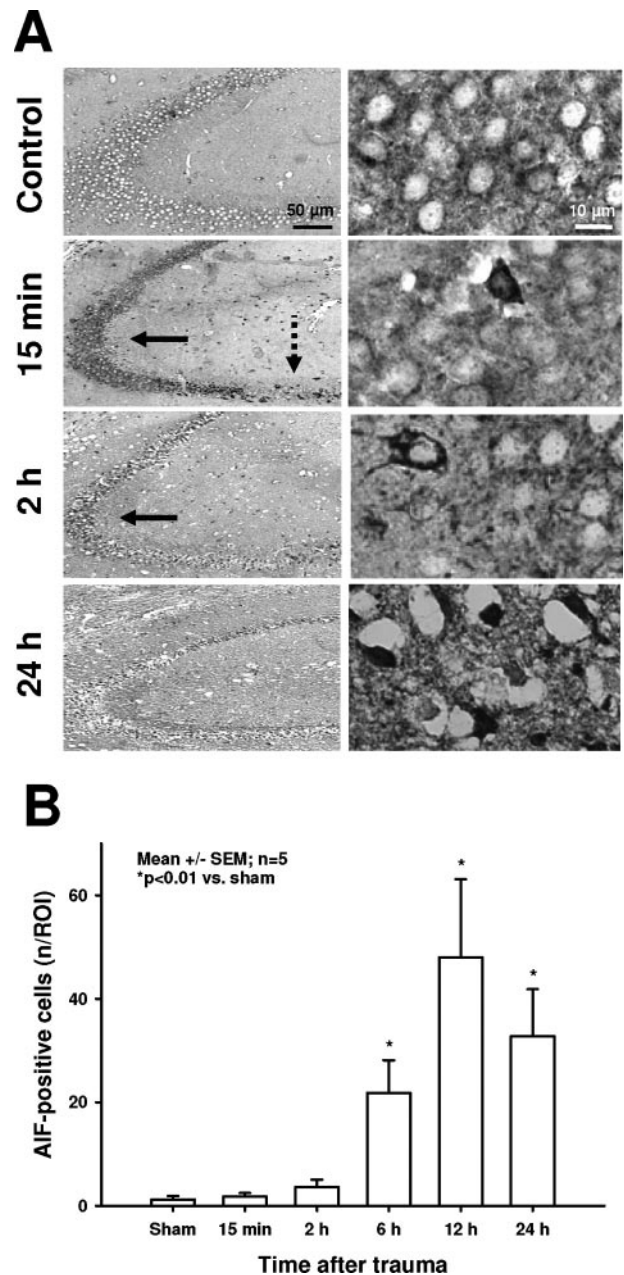


**Figure 4.** Nuclear translocation of AIF in the hippocampus following traumatic brain injury *in vivo*. **A:** Low- (left panels) and high-power (right panels) photomicrographs from uninjured control (upper left panel) and injured hippocampi. As in the cortex, AIF (dark staining) is detected only in the cytoplasm of control neurons (Control). At 15 minutes after trauma, the intensity of AIF staining increases in the cytoplasm of hippocampal neurons located toward the trauma site (arrow), while neurons further away from the injured cortex (upper left corner) do not show signs of AIF translocation (dotted arrow). At later time points, most neurons show nuclear AIF staining together with shrunken and serrated nuclei. **B:** Quantification of hippocampal cells (mean  $\pm$  SD) showing nuclear AIF staining (AIF positive) at different time points after TBI. Cell death in the hippocampus does not increase significantly until 6 hours after TBI ( $*P < 0.01$ ;  $n = 5$  per time point).

*in vivo*.<sup>29,36,37</sup> As already suggested by our *in vitro* data, the most prominent AIF staining was found in neurons (Figure 5, AIF+NeuN). Indeed, all cells showing strong AIF staining were also positive for the neuronal marker NeuN, indicating that astrocytes *in vivo* may express even less AIF than as suggested by our findings *in vitro*.

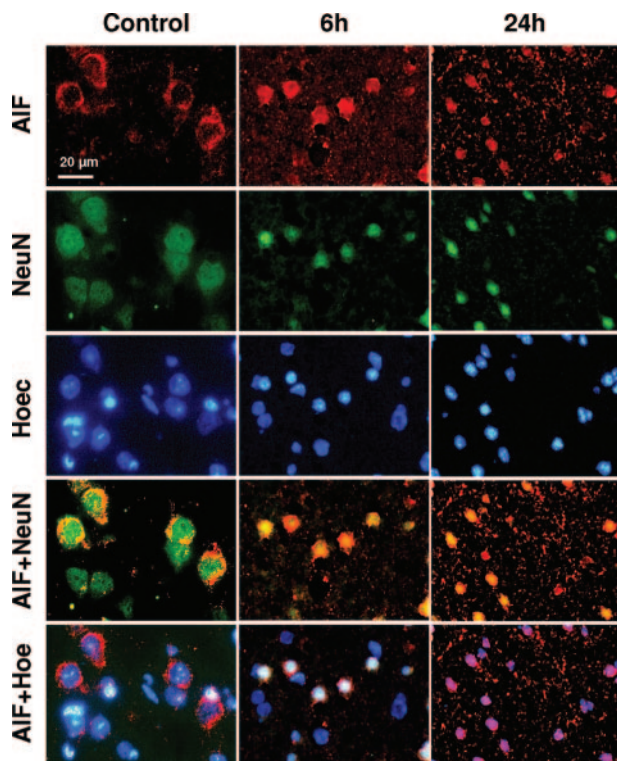


**Figure 5.** Trauma-induced nuclear translocation of AIF in the cerebral cortex is confined to neurons and associated with DNA damage and nuclear pyknosis. Immunohistochemistry of AIF (red), the neuronal marker NeuN (green), and the nuclear DNA-binding dye Hoe (blue). Under control conditions (Control), AIF was detected exclusively in the cytoplasm of neurons (AIF+Hoe). At 2, 6, and 24 hours after TBI, the overlay of AIF and Hoe (pink) indicate that AIF has translocated to the nucleus. At 6, and more clearly at 24 hours after trauma, the translocation of AIF is associated with nuclear pyknosis and cellular shrinkage.

After injury, AIF staining intensity increased almost immediately in the cytoplasm (Figures 3A and 4A, 15 minutes). A possible explanation for this rapid increase in AIF staining may be the better accessibility of the AIF protein to the applied antibody after release of AIF from mitochondria. At this time point, when most cortical and hippocampal neurons did not show any sign of nuclear damage, AIF staining was confined to the cytoplasm.

The first clearly nuclear AIF staining was observed in neurons surrounding the cortical contusion at 2 hours after trauma (Figure 3A, 2 hours). In contrast to pericontusional neurons, hippocampal neurons showed only cytoplasmic AIF staining at this time point (Figure 4A, 2 hours). Six hours after brain injury, the time when progressive pericontusional cell death has been shown to occur,<sup>11</sup> both cortical and hippocampal neurons showed nuclear localization of AIF, indicating translocation of AIF from mitochondria to the nucleus (Figures 3A and 4A, 6 hours). Nuclear translocation of AIF was mainly observed in cells showing advanced nuclear condensation and pyknosis, as demonstrated by double labeling of these cells with AIF and Hoechst 33342 (Figure 5, AIF+Hoe, 6 hours). Of note, all cells showing nuclear AIF staining were also positive for the neuronal marker NeuN, suggesting that AIF-mediated cell death occurs mainly in neurons (Figure 5, AIF+NeuN). At 24 hours after trauma,

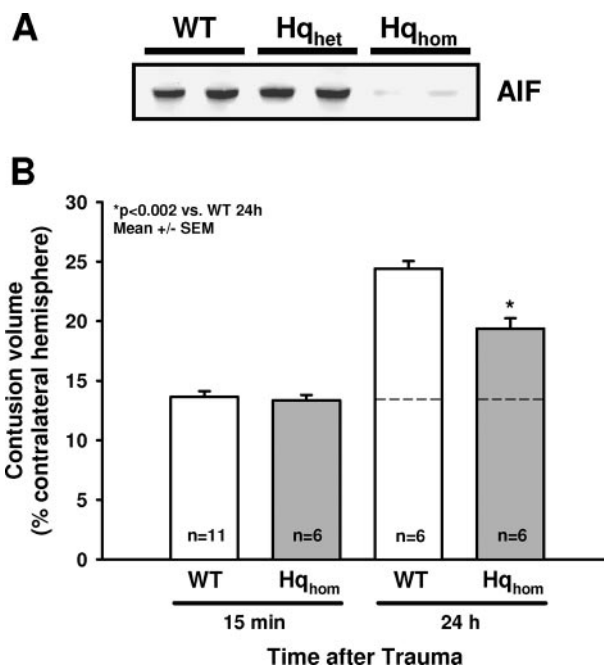


**Figure 6.** AIF-deficient mice have significantly less brain damage as compared to AIF-expressing control animals. **A:** Mice homozygously carrying the Hq AIF gene mutation express approximately 80% less AIF as compared to their wild-type littermates as determined by Western blot analysis. **B:** The contusion volume at 15 minutes after TBI in wild-type (+/+) mice represents the primary damage, and is determined only by the mechanical impact. The difference between the primary damage and the damage assessed after 24 hours represents the secondary damage. AIF-deficient (Hq/Hq) mice have a 44% reduced secondary brain damage (\* $P < 0.002$  vs. WT;  $n = 6$  to 11 per group).

most neurons in the traumatic penumbra showed advanced nuclear condensation and stained positive for nuclear AIF (Figure 5, 24 hours) indicating that AIF is involved in pericontusional neuronal cell death during the whole process of secondary contusion expansion.<sup>11</sup> These observations were substantiated by quantifying the number of cells displaying nuclear AIF staining in the pericontusional cerebral cortex and hippocampus (Figures 3B and 4B). In the cerebral cortex, the number of cells with nuclear AIF staining increased at 15 minutes postinjury ( $P < 0.01$  vs. control), whereas hippocampal neurons displayed significant nuclear AIF staining only at 6 hours after cortical impact. In both brain regions, the maximal number of AIF-positive cells was observed at 12 hours after trauma, a time course that fits well with the kinetics of delayed neuronal cell death following controlled cortical impact in mice.<sup>11</sup>

To investigate whether nuclear translocation of AIF plays a causal role in pericontusional cell death, we compared the contusion volumes of wild-type mice and Harlequin (Hq) mutant mice. Hq mice have a proviral insertion in the AIF gene resulting in deficient AIF expression; in other words, Hq mutant mice express only 20% of the AIF expressed by their wild-type littermates.<sup>36,42</sup> After confirming AIF-deficiency in Hq mice (Figure 6A), we subjected these animals and their wild-type littermates to controlled cortical impact injury. To assess the primary damage, we quantified the contusion volume in both wild-type and homozygous Hq mice at 15 minutes postin-



jury. To quantify which components resulted from secondary injury mechanisms, we also assessed contusion volumes at 24 hours after cortical impact injury.<sup>11</sup> Subtracting the primary contusion volume ( $13.6 \pm 1.6 \text{ mm}^3$ ) from the final contusion volume 24 hours after TBI ( $24.4 \pm 1.5 \text{ mm}^3$ ), we calculated the tissue volume that was damaged by secondary mechanisms to be  $10.8 \text{ mm}^3$  in wild-type mice, indicating that the primary contusion expanded by 79% (Figure 6B, white bars). In comparison, Hq mice showed a secondary contusion increase by only 45% (Figure 6B, gray bars), ie, a decrease of secondary brain damage by 44% ( $P < 0.002$ ).

## Discussion

The results of the current study show that AIF, a pro-apoptotic protein located inside the mitochondrial intermembrane space, is released from mitochondria, migrates to the nucleus, and is associated with nuclear condensation and caspase-independent neuronal cell death following stretch injury *in vitro* or traumatic brain injury *in vivo*. Specific down-regulation of AIF by siRNA in primary cultured neurons, or by a proviral insertion into the AIF gene in mice, resulted in a significant protection of injured neurons *in vitro*, and to a significant reduction of secondary contusion expansion *in vivo*, respectively. Therefore, the current findings suggest that AIF is a novel and significant mediator of post-traumatic neuronal cell death and that caspase-independent signaling pathways may play an important role in secondary brain injury following TBI.

## Expression of AIF in Cultured Cells and Brain Tissue

AIF shows a robust expression in primary cultured murine hippocampal neurons as demonstrated by co-immunolabeling of AIF and the neuronal marker MAP-2. This finding is corroborated by previous reports demonstrating expression of AIF in rat hippocampal cell lines and in primary cultured rat hippocampal and cortical neurons.<sup>36,37,43</sup> These *in vitro* findings are supported by our *in vivo* results, as well as by previous reports showing predominantly neuronal localization of AIF in the brain.<sup>28,29,36,37,41,43</sup> In the normal brain, AIF is located in the cytoplasm and co-localizes with the mitochondrial marker cytochrome oxidase,<sup>29,37</sup> thereby demonstrating that in neurons AIF is also located in mitochondria as was previously shown for non-neuronal cells.<sup>44</sup>

Although previous reports suggested predominantly neuronal expression of AIF *in vivo* (see above), we found also robust expression of AIF in cultured astrocytes as demonstrated by co-localization of AIF and glial fibrillary acidic protein, an astrocytic marker (Figure 1C). However, AIF staining in astrocytes could only be detected when using very high sensitivity settings for confocal microscopy, indicating that astrocytes express AIF at a much lower level as compared to neurons, a finding which may explain why AIF staining in astrocytes has been overlooked previously *in vivo*.

## Translocation of AIF from Mitochondria to the Nucleus after Traumatic Injury

AIF translocated from mitochondria to the nucleus at 24 hours following stretch injury to cultured neurons. This process was accompanied by nuclear condensation and axonal disruption, especially after moderate stretch (6.5 mm). The same degree of injury also resulted in loss of cell membrane integrity, as demonstrated by PI staining, and in significant loss of cell viability as quantified by FDA cleavage. Interestingly, astrocytes did not show any release of AIF from mitochondria or loss of viability after membrane stretch (data not shown), indicating that nuclear AIF translocation is indeed related to cell death and not an epiphenomenon of mechanical stress.

Previous reports have demonstrated that oxygen-glucose deprivation, toxic concentrations of glutamate, and exposure to free radicals also result in nuclear AIF translocation in neurons.<sup>28,36,37,43,45</sup> These data indicate that the release of AIF from mitochondria is not confined to mechanical cell damage, but also occurs independently of the initial mechanism of injury. This assumption is further supported by *in vivo* data showing that AIF translocates to the nucleus during post-traumatic cell death, as demonstrated in the current and in a previous study,<sup>28</sup> but also during neuronal cell death in experimental models of stroke, circulatory arrest-induced brain damage, and epilepsy.<sup>36,37,43,46</sup> Therefore, we propose that the release of AIF from mitochondria, followed by translocation to the nucleus, may be a common feature of different cell death pathways, and may represent a downstream and general mechanism of neuronal cell death. This assumption is most strongly supported by recent findings from our laboratory showing a very close temporal relationship between nuclear AIF translocation and cell death by real-time fluorescence video microscopy. Neurons become apoptotic several hours after a brief exposure to glutamate; AIF, however, is released from mitochondria and translocates to the nucleus only minutes before the nucleus becomes pyknotic and the cell disintegrates.<sup>47</sup>

## Prevention of Nuclear AIF Translocation after Traumatic Injury

To investigate whether nuclear translocation of AIF was indeed responsible for post-traumatic cell death, we reduced the expression of AIF in cultured neurons by addition of anti-AIF siRNA. This approach did not affect cellular protein expression in general, but specifically down-regulated AIF mRNA and protein by 70% to 80%, as shown previously.<sup>36</sup> siRNA-mediated down-regulation of AIF prevented cell death after moderate stretch (6.5 mm), and significantly reduced membrane damage to the level of mild injury, thereby demonstrating that AIF is a substantial player in cell death processes.

We further corroborated our *in vitro* data using mice with a proviral insertion in the AIF gene, resulting in a general reduction of AIF expression by over 80%.<sup>36,42</sup> When these mice and their wild-type littermates were subjected to experimental TBI, animals with reduced AIF

expression showed significantly reduced secondary brain damage as demonstrated by a 50% reduction of delayed contusion expansion. This degree of neuronal protection agrees well with our previous results using the same AIF-deficient mouse strain in other paradigms of acute brain injury, such as cerebral ischemia, epilepsy, and perinatal hypoxia-ischemia.<sup>36,41,46</sup>

### *Mechanisms of AIF Release from Mitochondria*

The precise mechanisms by which AIF is released from mitochondria in neurons are still under debate. Poly-ADP-ribose polymerase 1 was postulated to be an important upstream trigger of mitochondrial AIF release. This was elegantly demonstrated by the lack of mitochondrial AIF release following exposure of poly-ADP-ribose polymerase 1-deficient neurons to *N*-methyl-D-aspartate,<sup>48</sup> and by reduced AIF translocation and cell death following cerebral ischemia in mice treated with a specific Poly-ADP-ribose polymerase inhibitor.<sup>36</sup> Presumably, other downstream mechanisms of mitochondrial AIF release include the formation or prevention of mitochondrial membrane pores by members of the pro- or anti-apoptotic bcl-2 protein family. For instance, AIF translocation to the nucleus and neuronal cell death were previously shown to be reduced on pharmacological inhibition or siRNA-mediated down-regulation of the pro-apoptotic molecule Bid,<sup>36,47</sup> delivery of the anti-apoptotic molecule bcl-xl to the intracellular space, or overexpression of bcl-2.<sup>43,45</sup> Another mechanism of AIF release from mitochondria may be oxidative stress-induced permeabilization of the outer mitochondrial membrane as suggested for MPP+ (1-methyl-4-phenylpyridinium) toxicity in cultured dopaminergic neurons.<sup>49</sup> However, the potential role of intracellular or mitochondrial reactive oxygen species remains to be determined following stretch injury.

### *Mechanisms of AIF-Induced Cell Death*

The mechanisms of mitochondrial AIF release are of equal interest to the mechanisms by which AIF ultimately causes neuronal cell death. One of the most striking features of AIF-induced cell death is the necessity of AIF to interact with the nucleus. The addition of AIF to isolated nuclei induces pyknosis and large-scale (50 kDa) DNA fragmentation after 30 seconds.<sup>44</sup> Pyknosis is a hallmark of neuronal cell death *in vivo*, and AIF was found in pyknotic nuclei of neurons together with large scale DNA fragmentation following global cerebral ischemia, focal cerebral ischemia, and TBI<sup>29,37,43</sup> suggesting that AIF may be responsible for this process. Interestingly, AIF itself does not have any DNase activity, suggesting that AIF needs to associate with other factors to induce the changes described above. AIF does not depend on caspase activation and subsequent caspase-activated DNase (CAD/DFF45) activity to translocate to the nucleus and induce cell death,<sup>44,50</sup> a feature later also confirmed in neurons.<sup>51,52</sup> Recently, it was suggested that AIF induces DNA degradation only when it binds and translocates to the nucleus together with cyclophilin A (CypA), a

cytoplasmic protein known to be otherwise involved in immunomodulation.<sup>53</sup> These findings were extended to neurons in an *in vivo* model of perinatal hypoxia-ischemia, by demonstrating that CypA colocalizes with AIF in the nucleus of dying neurons, and by showing that CypA knock-out mice show significant neuroprotection associated with a lack of nuclear pyknosis and translocation of AIF to the nucleus.<sup>54</sup> The role that CypA may play in post-traumatic cell death remains to be elucidated.

Taken together, our results demonstrate that AIF mediates caspase-independent cell death following traumatic brain injury. Hence, inhibition of AIF-mediated cell death signaling may emerge as novel and efficacious therapeutic options for brain injured patients.

### *Acknowledgments*

The authors thank Ardeshir Ardeshiri, Uta Mamrak, Irina Eskina, Miriam Höhn, Jessica Livingston Thomas, Kevin Shaughnessy, and Ian Boswall for their excellent technical assistance.

### *References*

1. Langlois JA, Rutland-Brown W, Wald MM: The epidemiology and impact of traumatic brain injury: a brief overview. *J Head Trauma Rehabil* 2006, 21:375–378
2. Maas AI, Steyerberg EW, Butcher I, Dammers R, Lu J, Marmarou A, Mushkudiani NA, McHugh GS, Murray GD: Prognostic value of computerized tomography scan characteristics in traumatic brain injury: results from the IMPACT study. *J Neurotrauma* 2007, 24:303–314
3. Katayama Y, Mori T, Maeda T, Kawamata T: Pathogenesis of the mass effect of cerebral contusions: rapid increase in osmolality within the contusion necrosis. *Acta Neurochir Suppl* 1998, 71:289–292
4. Bullock R, Sakas D, Patterson J, Wyper D, Hadley D, Maxwell W, Teasdale GM: Early post-traumatic cerebral blood flow mapping: correlation with structural damage after focal injury. *Acta Neurochir Suppl (Wien)* 1992, 55:14–17
5. Unterberg AW, Stover J, Kress B, Kiening KL: Edema and brain trauma. *Neuroscience* 2004, 129:1021–1029
6. Bazan NG, Rodriguez de Turco EB, Allan G: Mediators of injury in neurotrauma: intracellular signal transduction and gene expression. *J Neurotrauma* 1995, 12:791–814
7. Sahuquillo J, Poca MA, Amorós S: Current aspects of pathophysiology and cell dysfunction after severe head injury. *Curr Pharm Des* 2001, 7:1475–1503
8. Raghupathi R: Cell death mechanisms following traumatic brain injury. *Brain Pathol* 2004, 14:215–222
9. Cervos-Navarro J, Lafuente JV: Traumatic brain injuries: structural changes. *J Neurol Sci* 1991, 103 Suppl: S3–S14
10. Zimmerman RA, Bilaniuk LT: Computer tomography of traumatic intracerebral hemorrhagic lesions: the change in density and mass effect with time. *Neuroradiology* 1978, 16:320–321
11. Zweckberger K, Eros C, Zimmermann R, Kim SW, Engel D, Plesnila N: Effect of early and delayed decompressive craniectomy on secondary brain damage after controlled cortical impact in mice. *J Neurotrauma* 2006, 23:1083–1093
12. Zipfel GJ, Babcock DJ, Lee JM, Choi DW: Neuronal apoptosis after CNS injury: the roles of glutamate and calcium. *J Neurotrauma* 2000, 17:857–869
13. Lewen A, Matz P, Chan PH: Free radical pathways in CNS injury. *J Neurotrauma* 2000, 17:871–890
14. Plesnila N, von Baumgarten L, Retiounskaia M, Engel D, Ardeshiri A, Zimmermann R, Hoffmann F, Landshamer S, Wagner E, Culmsee C: Delayed neuronal death after brain trauma involves p53-dependent inhibition of NF-kappaB transcriptional activity. *Cell Death Differ* 2007, 14:1529–1541

15. Morganti-Kossmann MC, Rancan M, Otto VI, Stahel PF, Kossmann T: Role of cerebral inflammation after traumatic brain injury: a revisited concept. *Shock* 2001, 16:165–177
16. Raghupathi R, Graham DI, McIntosh TK: Apoptosis after traumatic brain injury. *J Neurotrauma* 2000, 17:927–938
17. Wong J, Hoe NW, Zhiwei F, Ng I: Apoptosis and traumatic brain injury. *Neurocrit Care* 2005, 3:177–182
18. Eldadah BA, Faden AI: Caspase pathways, neuronal apoptosis, and CNS injury. *J Neurotrauma* 2000, 17:811–829
19. Yakovlev AG, Faden AI: Caspase-dependent apoptotic pathways in CNS injury. *Mol Neurobiol* 2001, 24:131–144
20. Qiu J, Whalen MJ, Lowenstein P, Fiskum G, Fahy B, Darwish R, Aarabi B, Yuan J, Moskowitz MA: Up-regulation of the Fas receptor death-inducing signaling complex after traumatic brain injury in mice and humans. *J Neurosci* 2002, 22:3504–3511
21. Bempohl D, You Z, Lo EH, Kim HH, Whalen MJ: TNF alpha and Fas mediate tissue damage and functional outcome after traumatic brain injury in mice. *J Cereb Blood Flow Metab* 2007, 27:1806–1818
22. Graham SH, Chen J, Clark RS: Bcl-2 family gene products in cerebral ischemia and traumatic brain injury. *J Neurotrauma* 2000, 17:831–841
23. Fiskum G: Mitochondrial participation in ischemic and traumatic neuronal cell death. *J Neurotrauma* 2000, 17:843–855
24. Robertson CL: Mitochondrial dysfunction contributes to cell death following traumatic brain injury in adult and immature animals. *J Bioenerg Biomembr* 2004, 36:363–368
25. Morita-Fujimura Y, Fujimura M, Kawase M, Chen SF, Chan PH: Release of mitochondrial cytochrome c and DNA fragmentation after cold injury-induced brain trauma in mice: possible role in neuronal apoptosis. *Neurosci Lett* 1999, 267:201–205
26. Sullivan PG, Keller JN, Bussen WL, Scheff SW: Cytochrome c release and caspase activation after traumatic brain injury. *Brain Res* 2002, 949:88–96
27. Penninger JM, Kroemer G: Mitochondria. AIF and caspases—rivaling for cell death execution. *Nat Cell Biol* 2003, 5:97–99
28. Zhang X, Chen J, Graham SH, Du L, Kochanek PM, Draviam R, Guo F, Nathaniel PD, Szabo C, Watkins SC, Clark RS: Intracellular localization of apoptosis-inducing factor (AIF) and large scale DNA fragmentation after traumatic brain injury in rats and in neuronal cultures exposed to peroxynitrite. *J Neurochem* 2002, 82:181–191
29. Zhu C, Qiu L, Wang X, Hallin U, Cande C, Kroemer G, Hagberg H, Blomgren K: Involvement of apoptosis-inducing factor in neuronal death after hypoxia-ischemia in the neonatal rat brain. *J Neurochem* 2003, 86:306–317
30. Slemmer JE, Matser EJ, De Zeeuw CI, Weber JT: Repeated mild injury causes cumulative damage to hippocampal cells. *Brain* 2002, 125:2699–2709
31. Slemmer JE, Weber JT: The extent of damage following repeated injury to cultured hippocampal cells is dependent on the severity of insult and inter-injury interval. *Neurobiol Dis* 2005, 18:421–431
32. Ellis EF, McKinney JS, Willoughby KA, Liang S, Povlishock JT: A new model for rapid stretch-induced injury of cells in culture: characterization of the model using astrocytes. *J Neurotrauma* 1995, 12:325–339
33. Slemmer JE, Weber JT, De Zeeuw CI: Cell death, glial protein alterations and elevated S-100 beta release in cerebellar cell cultures following mechanically induced trauma. *Neurobiol Dis* 2004, 15:563–572
34. McKinney JS, Willoughby KA, Liang S, Ellis EF: Stretch-induced injury of cultured neuronal, glial, and endothelial cells. Effect of polyethylene glycol-conjugated superoxide dismutase. *Stroke* 1996, 27:934–940
35. Weber JT, Rzigalinski BA, Willoughby KA, Moore SF, Ellis EF: Alterations in calcium-mediated signal transduction after traumatic injury of cortical neurons. *Cell Calcium* 1999, 26:289–299
36. Culmsee C, Zhu C, Landshamer S, Becattini B, Wagner E, Pellicchia M, Blomgren K, Plesnila N: Apoptosis-inducing factor triggered by poly(ADP-ribose) polymerase and Bid mediates neuronal cell death after oxygen-glucose deprivation and focal cerebral ischemia. *J Neurosci* 2005, 25:10262–10272
37. Plesnila N, Zhu C, Culmsee C, Groger M, Moskowitz MA, Blomgren K: Nuclear translocation of apoptosis-inducing factor after focal cerebral ischemia. *J Cereb Blood Flow Metab* 2004, 24:458–466
38. Plesnila N, Zinkel S, Le DA, Amin-Hanjani S, Wu Y, Qiu J, Chiarugi A, Thomas SS, Kohane DS, Korsmeyer SJ, Moskowitz MA: BID mediates neuronal cell death after oxygen/ glucose deprivation and focal cerebral ischemia. *Proc Natl Acad Sci USA* 2001, 98:15318–15323
39. Culmsee C, Gerling N, Lehmann M, Nikolova-Karakashian M, Prehn JH, Mattson MP, Krieglstein J: Nerve growth factor survival signaling in cultured hippocampal neurons is mediated through TrkA and requires the common neurotrophin receptor P75. *Neuroscience* 2002, 115:1089–1108
40. Zweckberger K, Stoffel M, Baethmann A, Plesnila N: Effect of decompression craniotomy on increase of contusion volume and functional outcome after controlled cortical impact in mice. *J Neurotrauma* 2003, 20:1307–1314
41. Zhu C, Wang X, Huang Z, Qiu L, Xu F, Vahsen N, Nilsson M, Eriksson PS, Hagberg H, Culmsee C, Plesnila N, Kroemer G, Blomgren K: Apoptosis-inducing factor is a major contributor to neuronal loss induced by neonatal cerebral hypoxia-ischemia. *Cell Death Differ* 2007, 14:775–784
42. Klein JA, Longo-Guess CM, Rossmann MP, Seburn KL, Hurd RE, Frankel WN, Bronson RT, Ackerman SL: The harlequin mouse mutation down-regulates apoptosis-inducing factor. *Nature* 2002, 419:367–374
43. Cao G, Clark RS, Pei W, Yin W, Zhang F, Sun FY, Graham SH, Chen J: Translocation of apoptosis-inducing factor in vulnerable neurons after transient cerebral ischemia and in neuronal cultures after oxygen-glucose deprivation. *J Cereb Blood Flow Metab* 2003, 23:1137–1150
44. Susin SA, Lorenzo HK, Zamzami N, Marzo I, Snow BE, Brothers GM, Mangion J, Jacotot E, Costantini P, Loeffler M, Larochette N, Goodlett DR, Aebersold R, Siderovski DP, Penninger JM, Kroemer G: Molecular characterization of mitochondrial apoptosis-inducing factor. *Nature* 1999, 397:441–446
45. Wang H, Yu SW, Koh DW, Lew J, Coombs C, Bowers W, Federoff HJ, Poirier GG, Dawson TM, Dawson VL: Apoptosis-inducing factor substitutes for caspase executioners in NMDA-triggered excitotoxic neuronal death. *J Neurosci* 2004, 24:10963–10973
46. Cheung EC, Melanson-Drapeau L, Cregan SP, Vanderluit JL, Ferguson KL, McIntosh WC, Park DS, Bennett SA, Slack RS: Apoptosis-inducing factor is a key factor in neuronal cell death propagated by BAX-dependent and BAX-independent mechanisms. *J Neurosci* 2005, 25:1324–1334
47. Landshamer S, Hoehn M, Barth N, Duvezin-Caubet S, Schwake G, Tobaben S, Kazhdan I, Becattini B, Zahler S, Vollmar A, Pellicchia M, Reichert A, Plesnila N, Wagner E, Culmsee C: Bid-induced release of AIF from mitochondria causes immediate neuronal cell death. *Cell Death Differ* 2008, 15:1553–1563
48. Yu SW, Wang H, Poitras MF, Coombs C, Bowers WJ, Federoff HJ, Poirier GG, Dawson TM, Dawson VL: Mediation of poly(ADP-ribose) polymerase-1-dependent cell death by apoptosis-inducing factor. *Science* 2002, 297:259–263
49. Chu CT, Zhu JH, Cao G, Signore A, Wang S, Chen J: Apoptosis inducing factor mediates caspase-independent 1-methyl-4-phenylpyridinium toxicity in dopaminergic cells. *J Neurochem* 2005, 94:1685–1695
50. Susin SA, Daugas E, Ravagnan L, Samejima K, Zamzami N, Loeffler M, Costantini P, Ferri KF, Irinopolou T, Prevost MC, Brothers G, Mak TW, Penninger J, Earnshaw WC, Kroemer G: Two distinct pathways leading to nuclear apoptosis. *J Exp Med* 2000, 192:571–580
51. Braun JS, Novak R, Murray PJ, Eischen CM, Susin SA, Kroemer G, Halle A, Weber JR, Tuomanen EI, Cleveland JL: Apoptosis-inducing factor mediates microglial and neuronal apoptosis caused by pneumococcus. *J Infect Dis* 2001, 184:1300–1309
52. Cregan SP, Fortin A, MacLaurin JG, Callaghan SM, Cecconi F, Yu SW, Dawson TM, Dawson VL, Park DS, Kroemer G, Slack RS: Apoptosis-inducing factor is involved in the regulation of caspase-independent neuronal cell death. *J Cell Biol* 2002, 158:507–517
53. Cande C, Vahsen N, Kouranti I, Schmitt E, Daugas E, Spahr C, Luban J, Kroemer RT, Giordanetto F, Garrido C, Penninger JM, Kroemer G: AIF and cyclophilin A cooperate in apoptosis-associated chromatinolysis. *Oncogene* 2004, 23:1514–1521
54. Zhu C, Wang X, Deinum J, Huang Z, Gao J, Modjtahedi N, Neagu MR, Nilsson M, Eriksson PS, Hagberg H, Luban J, Kroemer G, Blomgren K: Cyclophilin A participates in the nuclear translocation of apoptosis-inducing factor in neurons after cerebral hypoxia-ischemia. *J Exp Med* 2007, 204:1741–1748